Dalton Transactions

PAPER

View Article Online
View Journal | View Issue

Cite this: *Dalton Trans.*, 2014, **43**, 15950

Crystal structure, DFT, spectroscopic and biological activity evaluation of analgin complexes with Co(II), Ni(II) and Cu(II)†

Ahmed M. Mansour

Received 4th August 2014,
Accepted 28th August 2014

DOI: 10.1039/c4dt02366h

www.rsc.org/dalton

Reaction of analgin (NaL) with Co(II), Ni(II) and Cu(II) salts in ethanol affords complexes of the type [ML_2], which were characterized by elemental analysis, FT IR, UV-Vis, EPR, TG/DTA, magnetic susceptibility and conductance measurements. The copper(II) complex crystallizes in the orthorhombic *Pbca* space group. Analgin behaves as a mono-negatively tridentate ligand *via* pyrazolone O, sulfonate O and tertiary amino groups. The interaction of the tertiary nitrogen with M^{n+} ions is the main factor which determines the stability of complexes as revealed from natural bond orbital analysis data, where the binding energy of [ML_2] decreases with an increase in the bond length of the M–N bond. Time-dependent density functional theory calculations were applied in order to realize the electronic structures and to explain the related experimental observations. The anti-bacterial activity was studied on *Staphylococcus aureus* and *Escherichia coli*. Coordination of analgin to Ni(II) and Cu(II) leads to a significant increase in its antibacterial activity as compared with the Co(II) complex.

Introduction

Analgin (dipyrone, metamizole or novalgin) (Scheme 1) is the sodium salt of [(1,5-dimethyl-3-oxo-2-phenylpyrazol-4-yl)-methylamino]methanesulfonate. This drug presents antipyretic and analgesic activity[1] as well as other beneficial effects such as a vascular smooth muscle relaxant, anti-apoptotic, and anti-convulsant.[2] Analgin has both spasmolytic action and analgesic effect that makes it a favorable drug for colic pain.[3] However, the administration of analgin may be associated with severe effects such as chemical intolerance and agranulocytosis.[4]

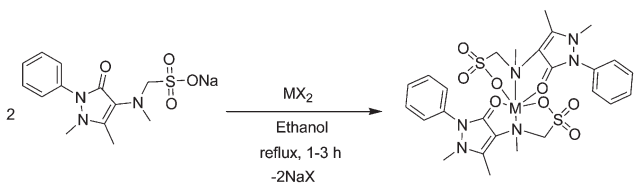

MX_2 = $Co(NO_3)_2{\cdot}6H_2O$ (**1**), $Ni(CH_3COO)_2{\cdot}4H_2O$ (**2**), and $Cu(NO_3)_2{\cdot}3H_2O$ (**3**)

Scheme 1 Synthesis of [ML_2] complexes (NaL = analgin drug).

Chemistry Department, Faculty of Science, Cairo University, Gamaa Street, Giza 12613, Egypt. E-mail: inorganic_am@yahoo.com, mansour@sci.cu.edu.eg; Fax: +20 2 35728843; Tel: +2 02 01222211253

†Electronic supplementary information (ESI) available. CCDC 986306. For ESI and crystallographic data in CIF or other electronic format see DOI: 10.1039/c4dt02366h

The mode of action involves the hydrolysis to 4-methyl-aminoantipyrine, with the latter further converted to other metabolites by various enzymatic reactions.[5] Analgin forms the active constituent of several drugs and a binary mixture with acetylsalicyclic acid and paracetamol. Several analytical techniques such as UV-Vis[6] and fluorescence spectroscopy,[7] HPLC,[8] flow injection analysis,[9] and polarography[10] were applied for the determination of analgin in the pharmaceuticals.

So far, pyrazolone and its derivatives were acknowledged to possess a wide range of industrial and pharmaceutical applications, which have attracted considerable scientific and applied interest.[11,12] Thus, it was essential for inorganic chemists to shed more light on the coordination behavior of analgin. To the best of my knowledge, no X-ray crystal data for metal complexes of analgin were reported in the literature, which makes the structures of these compounds ambiguous. Binary complexes of the type ML_2 (M = Co^{II}, Ni^{II}, Cu^{II}, and Zn^{II}) and $Cd(NaL)_2Cl_2$ were reported by Tatwawadi,[13] who assumed the interaction of analgin with M^{n+} as a bidentate ligand. Several mixed-ligand complexes of VO^{II}, Cr^{III}, Mn^{II}, Co^{III}, Ni^{II}, Mo^{II}, $WO_2{}^{VI}$, and Hg^{II} metal ions were also synthesized and characterized by Maurya *et al.*[14] supposing that analgin coordinated through only the pyrazolone O atom. Besides, the reaction between analgin and Fe^{III} in the presence of different anions was followed by means of UV, IR, and pH-metric titrations.[15] The composition and stability of Hg^{II} complexes were pH-metrically studied,[16] where the development of

complexes assumed to proceed through only the pyrazole ring O and SO_3 group.

The search for new effective antimicrobial agents is of paramount importance, but the discovery of new drugs having completely new chemical structures is time consuming and expensive. Thus, molecular structure modification is better and desirable. Analgin presents a chemical structure that favors chemical modifications by means of complexation with some transition metal ions. In the present study, Co(II), Ni(II) and Cu(II) complexes of the analgin antipyretic drug were synthesized, characterized, and tested for their biological activity against *Staphylococcus aureus* and *Escherichia coli*. Structural properties have been studied both experimentally and theoretically and are correlated here. Natural bond orbital (NBO) analysis has also been performed to provide details of the type of hybridization and the nature of bonding in the studied complexes. With the aim of understanding the electronic structures of the complexes and the related experimental observations, TD-DFT calculations were applied.

Results and discussion

Structural characterization

The reaction of $Co(NO_3)_2{\cdot}6H_2O$, $Ni(CH_3COO)_2{\cdot}4H_2O$, and $Cu(NO_3)_2{\cdot}3H_2O$ with two equivalents of analgin in ethanol affords pink (**1**), blue (**2**) and crystalline green (**3**) complexes of the type $[ML_2]$ in that order (Scheme 1). These complexes were characterized by elemental analysis, TG/DTA, IR, EPR, UV-Vis, and magnetic and conductance measurements. However, unambiguous proof of the tridentate behavior of analgin *via* pyrazolone O, sulfonate O and tertiary amino group to the metal ions finally came from the single crystal X-ray analysis of complex **3**. Relevant parameters are listed in Table 1 and the molecular structure of $[CuL_2]$ is shown in Fig. 1. Among the various vibrational bands of analgin, studies of the C=O, C–N, and SO_3 modes were found to be useful in determining the coordination sites. The FT IR spectrum of analgin showed a strong C=O stretching band at 1660 cm^{-1}, which shifted to a lower wave number, 1604 (**1**), 1611 (**2**), and 1600 (**3**), suggesting the participation of the C=O group in the coordination sphere of the metal ions. The assignment of the stretching bands of the C–N and SO_3 groups in the region between 1400 and 1000 cm^{-1} is not easily interpreted owing to their overlap with the aromatic bands. Therefore, it was necessary to compare first the spectrum of analgin with that of phenazole, which have a similar structure, but without attaching the $-N(CH_3)CH_2SO_3Na$ group to position 4 of the pyrazolone ring. In general, the non-coordinated anionic SO_3 shows two bands due to the asymmetric and symmetric stretching modes.[17] On coordination to the metal ion, three ν(SO) bands are observed as the C_{3v}-symmetry is broken. Comparison of analgin with phenazole showed two new bands at 1182 and 1051 cm^{-1} assigned to ν^{ss}(SO), while the asymmetric mode is overlapped. In complexes, the SO_3 group gave rise to a doublet structure at (1265, 1166) (**1**), (1263, 1169) (**2**), and (1245, 1196 cm^{-1}) (**3**) corresponding to asymmetric and symmetric modes.[18] In addition, the ν^{ss}(SO) at 1051 cm^{-1} in analgin was shifted to 1019 (**1**), 1022 (**2**), and 1030 cm^{-1} (**3**) suggesting the contribution of SO_3 in the complex formation. The ν(C–N) in the uncoordinated analgin was found at 1343 cm^{-1}, and shifted to ≈1331 cm^{-1} in complexes. The most noteworthy observation is that the anion of the metal salt has no role in the complex formation, as the IR spectra of the complexes which were pre-

Table 1 Crystal data and structure refinement for **3**

Molecular formula	$C_{26}H_{32}CuN_6O_8S_2$
Formula weight	684.25
Crystal system	Orthorhombic
Space group	*Pbca*
Color	Green
Wavelength (Å)	0.7107
Unit cell dimensions (Å, °)	
a	10.607(2) Å
b	15.644(3) Å
c	17.786(4) Å
α	90.00°
β	90.00°
γ	90.00°
V	2951.3 (10) $Å^3$
Z	4
T (K)	298
D_x (g cm^{-3})	1.540
Absorption coefficient (mm^{-1})	0.941
F(000)	1420.0
Theta range for collection	27.478–2.910
Index range	$h = 0 \rightarrow 13$, $k = 0 \rightarrow 20$, $l = 0 \rightarrow 23$
Absorption correction	Multi-scan
Max. and min. transmission	0.708 and 0.589
Minimum/maximum transmission	0.613/0.403
Refinement method	Full matrix least squares on F^2
Criterion	$I > 2.00\sigma(I)$
Data/parameters/restraints	3339/199/0
Goodness of fit on F^2	1.029
R(all)	0.0904
R(gt)	0.0458
w*R*(ref)	0.1279
w*R*(gt)	0.1079
Reflections (all)	3339
Reflections (gt)	2072

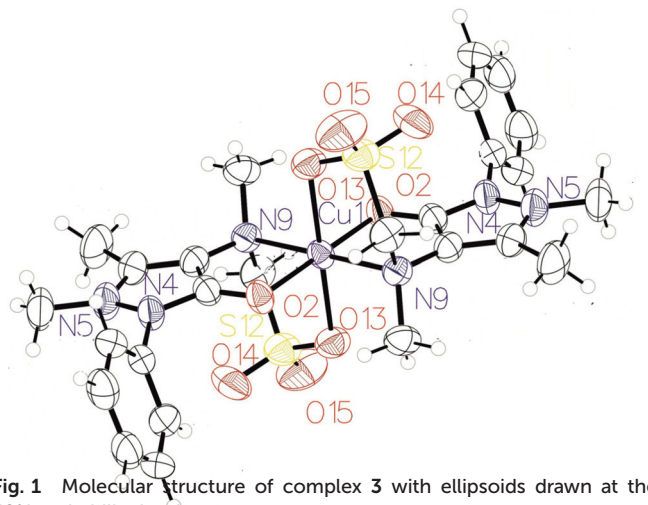

Fig. 1 Molecular structure of complex **3** with ellipsoids drawn at the 50% probability level.

pared from either the chloride or acetate salts are typical. Therefore, analgin behaves as a N,O,O tridentate ligand towards M^{n+} ions.

For complexes **1** and **3**, the thermal decompositions start from 270 and 236 °C with a continuous weight loss in the temperature range of 270–546 and 236–561 °C respectively. Three endothermic stages at 253, 383, and 513 °C for **1** and at 220, 269, and 478 °C for **3** were identified and assigned to organic ligand decomposition with high percentage of the final residues (18.24% for **1** and 16.37% for **3**) at 1100 °C. The final residue may be considered to be CoS_2 (calcd 17.99%; **1**) and carbonized CuS (calcd 15.72%; **3**).[19] The simultaneous TG/DTA of **2** showed that the thermal decomposition takes place *via* three complicated stages maximized at 274, 411, and 475 °C. These steps bring the total mass loss up to 88.73% of the parent complex. Such mass loss is close to the calculated value (89.08%) expected for the formation of NiO as a final residue.

Electronic structure, magnetic and EPR measurements

The crystal field theory of high spin octahedral Co(II) complexes[20] predicted three spin allowed d–d transitions, namely $^4T_{1g}\rightarrow{}^4T_{2g}(F)$ (ν_1), $^4T_{1g}\rightarrow{}^2A_{2g}$ (ν_2) and $^4T_{1g}\rightarrow{}^4T_{2g}(P)$ (ν_3). The electronic spectrum of **1** showed only one band in DMSO at 275 nm as well as a shoulder at 420 nm assigned to the π–π*/aromatic system and n–π*(C═O)/$^4T_{1g}\rightarrow{}^4T_{2g}(P)$ (ν_3), respectively. The effective magnetic moment (μ_{eff}) of 4.71μ_B for complex **1** further complements the electronic spectral findings as this value lies in the acceptable experimental range (4.10–5.20μ_B) for high spin cobalt(II) complexes.[21] The electronic ground state of octahedral Ni(II) complexes is $^3A_{2g}$ and three spin-allowed transitions: $^3A_{2g}\rightarrow{}^3T_{2g}$ (ν_1), $^3A_{2g}\rightarrow{}^3T_{1g}(F)$ (ν_2), and $^3A_{2g}\rightarrow{}^3T_{1g}(P)$ (ν_3) are expected.[22] Some octahedral Ni(II) complexes[23] showed a weak broad band at about 790 nm corresponding to the spin-forbidden $^3A_{2g}\rightarrow{}^1E_g$ transition. Complex **2** displayed three bands in DMSO at 275, 400 and 535 nm assigned to the internal ligand transitions, MLCT/n–π* (C═O) and $^3A_{2g}\rightarrow{}^3T_{1g}$ (F) (ν_2), respectively, in an octahedral geometry. The μ_{eff} of **2** is found to be 3.70μ_B (298 K) in the presence of spin–orbital coupling.[24] This value exceeds the spin-only value, but is not as high as μ_{s+L}.[21] This happens because the electric fields of atoms, ions, and molecules surrounding the metal ion in its compounds restrict the orbital motion of the electrons so that the orbital angular momentum and hence the orbital moments are partially quenched. For octahedral Cu(II) complexes, it has been established that the split of ^2E_g and $^2T_{2g}$ states of the ^2D ground state may keep the three $^2B_{1g}\rightarrow{}^2A_{1g}$ (ν_1), $^2B_{1g}\rightarrow{}^2B_{2g}$ (ν_2) and $^2B_{1g}\rightarrow{}^2E_g$ (ν_3) electronic transitions unresolved in the spectra of the elongated tetragonal or rhombic distortion (D_{4h} symmetry) geometries. Complex **3** showed four bands in DMF at 270, 375, 485, and 780 nm. The broad band at 780 nm can be assigned in terms of overlapping of the ν_1–ν_3 bands in an octahedral geometry. The band at 485 nm has LMCT character, which may be originated from the SO_3 group, while those at 270 and 375 nm are attributed to π–π*/aromatic and n–π*(C═O), respectively. The μ_{eff} of **3**, corrected for diamagnetic and temperature-independent paramagnetic contributions, is 2.57μ_B (298 K). This value is higher than the spin-only value expected for non-interacting Cu^{II} ions ($S = 1/2$, $t_{2g}^6e_g^3$), but is in the acceptable range for Cu(II) complexes.[21]

The X-band EPR spectrum of **3** in the solid state (Fig. 2) at 298 K exhibits typical four line noticeable $^{63/65}Cu$ ($I = 3/2$) hyperfine splitting with $g_{\|} = 2.320$ ($A_{\|} = 143 \times 10^{-4}$ cm^{-1}) and $g_{\perp} = 2.074$ characteristic of mononuclear copper(II) complexes having rhombic-octahedral with the elongation of the axial bonds or square-based pyramidal symmetries and $d_{x^2-y^2}$ orbital in the ground state. This spectrum is usually obtained with a large ligand like analgin that increases the Cu–Cu distance and decreases the line width.[25] The geometric parameter G, which is a measure of the exchange of interactions between the copper centers in a powdered sample, has been calculated[26] as $G = (g_{\|} - 2.0023)/(g_{\perp} - 2.0023)$. According to Hathaway[27] if $G > 4$, the exchange interaction is negligible and

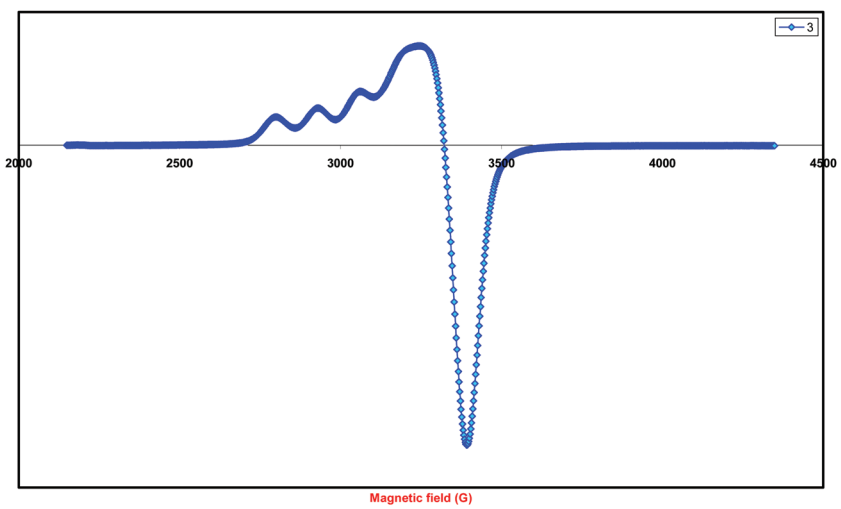

Fig. 2 EPR spectrum of complex **3**.

$G < 4$ indicates exchange interaction. The value of G is found to be 4.32 indicating the absence of moderate exchange interactions among the copper molecules in the solid state.

Crystal structure

X-ray single-crystal diffraction data revealed that complex **3** crystallizes in the orthorhombic *Pbca* space group. A view of the molecular structure of **3** is shown in Fig. 1. Selected crystallographic data are presented in Table 2. The six-coordinated Cu(II) ion is arranged in a slightly distorted octahedral geometry, where two analgin molecules lying in a *trans*-conformation are acting as tridentate chelators forming four stable five-membered rings. An inversion centre of symmetry is found at the copper atom, where the two ligands are adjusted in a linear way, but pointing in opposite directions. The structure is coplanar, where the bond angles O2–Cu–O2^{i}, N9–Cu–N9^{i}, and O13–Cu–O13^{i} equal 180°. The coordination sphere consists of two pyrazolone oxygen atoms [CuO2 = 2.007(2) Å], two N atoms [CuN9 = 2.009(2) Å] and two oxygen atoms [CuO13 = 2.321(2) Å] of SO_3 groups. The two covalent Cu–O13 bond lengths are equal, but they are longer than the Cu–O2 bond distances. As shown in Table 2, the distortion around the copper atom is low, where the bond angles are slightly deviating from those of a regular octahedron. In the crystal packing, it is possible to observe π–π stacking interactions between the ring planes (Fig. 3a), and also the molecules are cross-linked to each other through $O_2SO\cdots H–C$ with a distance of 2.734 Å (Fig. 3b).

Table 2 Selected experimentally determined bond lengths (Å) and angles (°) for complex **3**

Bond length (Å)		Angles (°)	
Cu–O2	2.007 (2)	O2–Cu–O2^{i}	180.00 (5)
Cu–O2^{i}	2.007 (2)	N9–Cu–N9^{i}	180.00 (13)
Cu–N9	2.099 (2)	O13–Cu–O13^{i}	180.00 (5)
Cu–N9^{i}	2.099 (2)	O2–Cu–N9	87.66 (8)
Cu–O13	2.321 (2)	O2–Cu–O13	92.17 (9)
Cu–O13^{i}	2.321 (2)	N9–Cu–O13	83.71 (9)
		O2–Cu–O13^{i}	87.82 (9)
		O2–Cu–N9^{i}	92.34 (8)
		N9–Cu–O13^{i}	96.29 (9)

DFT/TD-DFT

To obtain an insight into the geometrical and electronic structures of the investigated complexes, [ML_2] (M = Co(II), Ni(II), and Cu(II)) were optimized (Fig. S1†) at the DFT/B3LYP level of theory starting from the X-ray structure coordinates of the Cu(II) complex. The complexes were characterized as local minima through harmonic frequency analysis. Selected calculated bond lengths and angles are compared in Table S1.† Good agreement was found for the Cu–O bonds, while the value of the Cu–N bond is overestimated by the DFT method. The M–N bond distance increases from Ni to Co and then Cu. The bond angles slightly differ by 2–3°. This happens because the calculations are performed in the gaseous state, whereas packing molecules with inter- and intra-molecular interactions are treated in the experimental measurements. The nature of the electronic transitions observed in the UV-Vis spectra of the complexes has been studied by time-dependent DFT. The lowest 30 singlet-to-singlet spin-allowed excitation states were calculated using the same functional and basis set for the geometry optimization. In the model structures of the investigated complexes, to reduce the computer time, the phenyl ring and two methyl groups attached to the pyrazolone ring were replaced by H atoms. The calculated d–d excitation wavelengths, energies of other excitation transitions ($f > 0.002$) and their assignments are tabulated in Table S2.† As expected, the d–d transitions are forbidden and their oscillator strengths are also close to 0.0. In the 320–800 nm region, the stimulated spectrum of the Co(II) complex showed three forbidden transitions at 761, 533 and 484 nm as well as a highest energy band at 335 nm corresponding to H(β) → L+2(β), H(β) → L+5(β), H−1(β) → L+5(β) and H(β) → L(β) (H: HOMO and L: LUMO). The HOMOs are mainly composed of Co d character, and the LUMO orbital is of Co d_{z^2}nature (Table S3†). The transition energy at 761 nm has a ground state composed of Co d character, whereas the excitation state is of pyrazolone π* orbitals forming a MLCT. Similarly, the low oscillator strength

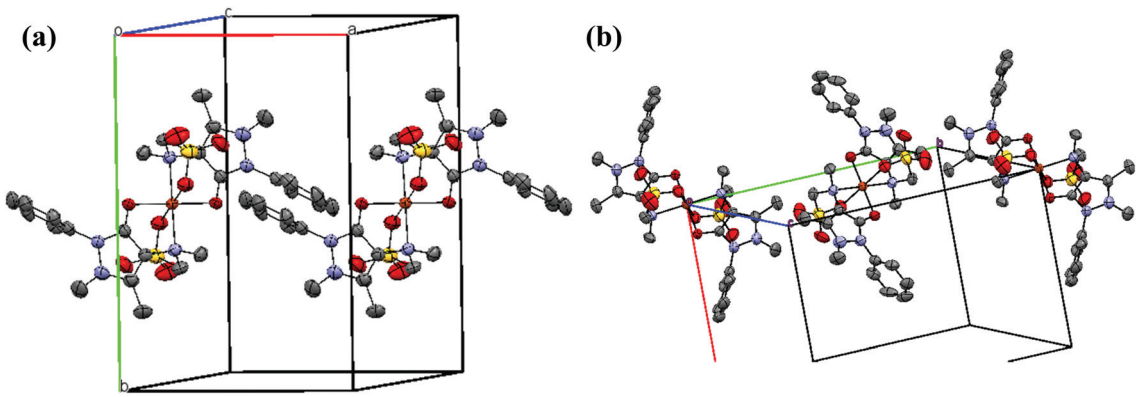

Fig. 3 (a) A view showing the π–π stacking interactions of the phenyl rings; (b) cross-linking of copper complexes to each other through O2SO···H–C.

transitions at 533 and 484 nm are MLCT to the π* system of the SO_3 groups. The band at 335 nm can be assigned to $d_{xz} \rightarrow d_{z^2}$ in an octahedral structure. The HOMO–LUMO gap in **1** is 4.22 eV, which is higher than that of **2**. The TD-DFT spectrum of **2** displayed three transitions at 484, 415 and 409 nm with oscillator strengths of 0.0002, 0.0017, and 0.0011, respectively. HOMO and HOMO−1 show predominantly 3d character. HOMO−4, which is lower than HOMO by 3.65 eV, results from the π system of the pyrazolone rings (Table S4†). The two LUMOs (LUMO and LUMO+1) are lying close to HOMO with a small energy gap (0.81 eV) between HOMO and LUMO. These orbitals are a mixture of π* orbitals resulting from the two coordinated pyrazolone moieties. Hence, the electronic transitions: H−1 → L (484 nm)/H → L+1 (409 nm) and H−4 → L (415 nm) are MLCT and π–π* characters, respectively. The calculated spectrum of **3** is characterized by three lowest energy electronic transitions at 809, 569, and 526 nm assigned to H(β) → L, H−1(β) → L, and H−3(β) → L, respectively. As shown in Fig. 4, the MOs from HOMO−3 to LUMO are mainly of Cu d character and energetically well separated from the next lower occupied MOs. The LUMO orbital with β-spin is mainly of Cu d_{z^2} character, whereas the HOMO orbital is coming from the Cu d_{xy}. Hence, the electronic transition at 809 nm is assigned to $d_{xy} \rightarrow d_{z^2}$ characteristic of the octahedral Cu(II) complexes.

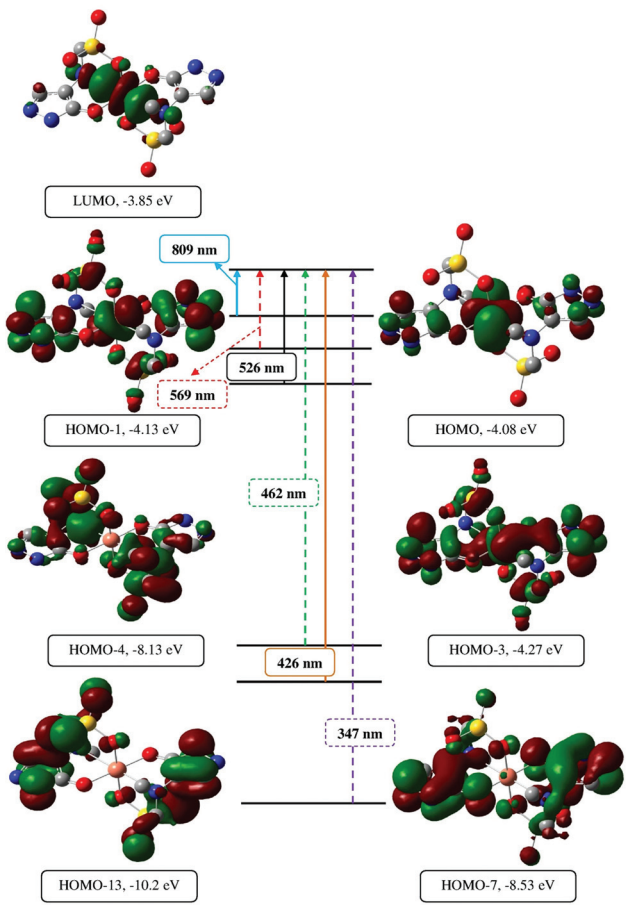

Fig. 4 Theoretical electronic absorption transitions of complex **3**.

The bands at 569 and 526 nm are of LMCT character, originating from the pyrazolone rings and SO_3 groups and going to Cu d_{z^2}. The highest energy bands at 462, 426, and 347 nm with significant oscillator strengths are all of π–π* character.

Natural bond orbital (NBO) analysis

According to NBO,[28] the electronic arrangement of Co in **1** is: $[Ar]4s^{0.20}3d^{7.56}4p^{0.41}4d^{0.01}5p^{0.01}$ with 8.167 valence electrons. The occupancies of Co 3d are: $d_{xy}^{1.858}$ $d_{xz}^{0.751}$ $d_{yz}^{1.736}$ $d_{x^2-y^2}^{1.421}$ $d_{z^2}^{1.794}$. The calculated natural charge was found to be 0.821 as a result of electron density donation from two tridentate molecules. Similarly, the electronic configuration of the Ni atom in **2** is $[Ar]4s^{0.20}3d^{8.60}4p^{0.39}5p^{0.01}$ with about one electron more in the d sub-shell (9.189) compared with complex **1**, indicating that the quantity of the electron density donation from the two ligands is the same or slightly more excess in the Ni^{II} center. The occupancies of Ni 3d are: $d_{xy}^{1.984}$ $d_{xz}^{1.512}$ $d_{yz}^{1.919}$ $d_{x^2-y^2}^{1.326}$ $d_{z^2}^{1.857}$. For complex **3**, the electronic arrangement of Cu is $[Ar]4s^{0.24}3d^{9.33}4p^{0.37}5p^{0.01}$ distributed as 18 core electrons, 9.935 valence electrons (on 4s, 3d, and 4p atomic orbitals) and 0.010 Rydberg electrons (mainly on the 5p orbital) giving a total of 27.945 electrons and leaving 1.053. The occupancies of Cu 3d are: $d_{xy}^{1.985}$ $d_{xz}^{1.529}$ $d_{yz}^{1.873}$ $d_{x^2-y^2}^{1.965}$ $d_{z^2}^{1.973}$. The strength of interactions between the metal ion and donor sites can be estimated by the second order perturbation theory. The larger the E^2 value, the more intensive is the interaction between electron donors and electron acceptors. For complex **1**, the E^2 values are 290, 120, and 280 cal mol^{-1} for LP(2)-O2→RY*(2)Co/LP(2)O39→RY*(2)Co, LP(1)N4→RY*(2)Co/LP(1)-N41→RY*(2)Co and LP(3)O5→RY*(2)Co/LP(3)O43→RY*(2)Co, in that order. These M–L interactions have energies of 230, 490, and 70 cal mol^{-1} in **2**, and 420, 30 and 120 cal mol^{-1} in complex **3**, respectively. Binding energies are defined as the total energy of the complex minus the sum of total energies of the most stable isolated moieties.[29] Complex **2** is more stable than **1** by ≈2.813 kcal mol^{-1} and than **3** by 22.615 kcal mol^{-1}. Thus, the stronger the binding capability is, the more stable the complex will be, and the higher the metal binding selectivity of a ligand to the metal ions will be. The interaction of the tertiary nitrogen with M^{n+} is the main factor determining the stability of the studied complexes, where the binding energy decreases with an increase of the M–N bond distance.

Antibacterial activity

The antimicrobial activities of analgin and its complexes were studied using two microbes *S. aureus* and *E. coli* and compared to tetracycline which was used as a standard. Preliminary screening was carried out at 20 mg mL^{-1}. In classifying the antibacterial activity as Gram-positive or Gram-negative, it would be expected that a much greater number of drugs would be active against Gram-positive than Gram-negative bacteria.[30] Analgin showed lower activity against *S. aureus* (G^+) than tetracycline, and was inactive against *E. coli*. It is clear from the inhibition zone diameter data of the investigated complexes that the antibacterial activity of analgin is affected by the type of the divalent cation. Coordination of analgin to Co(II) did not

alter the toxicity, but the formation of complexes **2** and **3** results in excellent activity against the resistant *E. coli* (G^-), as well as *S. aureus* bacterium. The activity of **2** and **3** did not discriminate between the tested organisms. The higher toxicity of **2** and **3** can be explained by Tweedy's chelation theory,[31] which explicated that the lipophilicity of the free organic ligand is changed by reducing the polarizability of the M^{n+} ion *via* the L→M donation, and the possible electron delocalization over the complexes. Lipophilicity is an important factor associated with the membrane permeation in biological systems: the higher the lipophilicity, the easier the penetration in the cell through the cellular membrane.

Conclusion

Co(II), Ni(II), and Cu(II) complexes of the analgin antipyretic drug were prepared in good yields, characterized, and tested for their biological activity against *S. aureus* and *E. coli*. Unequivocal proof of the tridentate nature of analgin came from the X-ray crystallography data. The M(II) ion is arranged in a slightly distorted octahedral geometry, where two analgin molecules are acting as tridentate chelators forming four stable five-membered rings. The experimental studies were complemented by quantum chemical calculations. Coordination of analgin to Co(II) did not alter the toxicity, but the formation of Ni(II) and Cu(II) complexes results in excellent activity against the tested organisms.

Experimental

Synthesis of complexes

Instruments. FT IR spectra were recorded as potassium bromide pellets using a Jasco FTIR 460 plus in the range of 4000 to 200 cm^{-1}. Elemental microanalysis was performed using Elementer Vario EL III. TG/DTA analysis was performed under a nitrogen atmosphere (20 mL min^{-1}) in a platinum crucible with a heating rate of 10 °C min^{-1} using a Shimadzu DTG-60H simultaneous DTG/TG apparatus. Magnetic measurement was carried out on a Sherwood scientific magnetic balance using the Gouy method,[30] and $Hg[Co(SCN)_4]$ was used as a calibrant. Electronic spectra were scanned on a Shimadzu Lambda 4B spectrophotometer in both DMSO and DMF solutions. A digital Jenway 4310 conductivity meter with a cell constant of 1.02 was used for the molar conductance study. X-band EPR measurements were performed on solid samples at 298 K using a Bruker EMX spectrometer. The magnetic modulation frequency was 100 kHz and the microwave power was set to 0.201 mW. The *g*-values were obtained by referencing to a diphenylpicrylhydrazyl (DPPH) sample with g = 2.0036. The modulation amplitude was set at 4 Gauss while the microwave frequency was determined as 9.775 GHz.

Synthesis. Two mmol of analgin (646 mg) and one mmol of $Co(NO_3)_2{\cdot}6H_2O$ (291 mg), $Ni(CH_3COO)_2{\cdot}4H_2O$ (248 mg), or $Cu(NO_3)_2{\cdot}3H_2O$ (241 mg) were dissolved in ethanol (15 mL) and heated to reflux (1–3 h), where pink Co(II) (**1**), blue Ni(II) (**2**) and crystalline green Cu(II) (**3**) complexes were precipitated. Diffusion of analgin solution to Cu^{2+} ions in ethanol gave green crystals suitable for X-ray structure analysis. Lower molar conductance values (in DMF) were reported for the complexes compared with the reported values[32] for 1 : 1 (65–90 Ω^{-1} cm^2 mol^{-1}) and 1 : 2 (130–170 Ω^{-1} cm^2 mol^{-1}) electrolytes in DMF, indicating their non-electrolytic nature.

• Complex **1** ($C_{26}H_{32}CoN_6O_8S_2$): Yield: 73%: %Calcd (%Found). C, 45.95 (45.48); H, 4.75 (4.77); N, 12.37 (12.63). FT IR: 1604, ν(C═O); 1331, ν(C–N); 1256 ν^{ass}(S–O); 1166 ν^{ss}(S–O); and 1019 ν^{ss}(S–O) cm^{-1}. UV-Vis (DMF): 275 and 420 nm. μ_{eff} = 4.71μ_B (298 K). Molar Cond. (10^{-3} M, DMF): 13.51 Ω^{-1} cm^2 mol^{-1}.

• Complex **2** ($C_{26}H_{32}N_6NiO_8S_2$): Yield: 77%: %Calcd (%Found). C, 45.96 (45.39); H, 4.75 (4.78); N, 12.37 (13.50). FT IR: 1611, ν(C═O); 1331, ν(C–N); 1263 ν^{ass}(S–O); 1169 ν^{ss}(S–O); and 1022 ν^{ss}(S–O), cm^{-1}. UV-Vis (DMF): 275, 400 and 535 nm. μ_{eff} = 3.70μ_B (298 K). Molar Cond. (10^{-3} M, DMF): 13.01 Ω^{-1} cm^2 mol^{-1}.

• Complex **3** ($C_{26}H_{32}CuN_6O_8S_2$): Yield: 68%: %Calcd (%Found). C, 45.64 (44.80); H, 4.71 (4.64); N, 12.28 (12.27). FT IR: 1600, ν(C═O); 1331, ν(C–N); 1245 ν^{ass}(S–O); 1196 ν^{ss}(S–O); and 1030 ν^{ss}(S–O), cm^{-1}. UV-Vis (DMF): 270, 375, 485 and 780 nm. μ_{eff} = 2.57μ_B (298 K). Molar Cond. (10^{-3} M, DMF): 18.12 Ω^{-1} cm^2 mol^{-1}.

X-ray diffraction analysis

Crystallographic data were collected on an Enraf-Nonius CAD4 single crystal X-ray diffractometer with graphite monochromated Mo-K_α radiation (λ = 0.71073 Å) at 298 K. All the diffracted intensities were corrected for Lorentz-polarization and absorption.[33,34] The structure was solved using the SIR92[35] computer program in the space group *Pbca* and then refined with the SHELX software package.[36] All hydrogen atoms were included in calculated positions. The figures involving hydrogen-bonds and packing were drawn using Mercury.[37] Crystallographic data have been deposited with the Cambridge Crystallographic Data Center as supplementary publication no. CCDC 986306 for complex **3**.

DFT calculations

Geometry optimizations of complexes **1–3** in the gas phase were carried out by the DFT/B3LYP method combined with the LANL2DZ basis set[38] using Gaussian 03,[39] where the singlet state was assigned to complex **2** and the doublet state to both **1** and **3**. The starting geometry for optimization was constructed based on crystallographic data without any symmetry restriction. The complexes were characterized as local minima through harmonic frequency analysis. Electronic transitions were calculated by TD-DFT.[40] Natural bond orbital (NBO) analysis and the analysis of frontier molecular orbitals were performed at the same level of theory.

Antibacterial activity

The antimicrobial activities of the test samples were determined by a modified Kirby–Bauer disc diffusion method[41]

under standard conditions using Mueller-Hinton agar medium (tested for composition and pH), as described by NCCLS.[42] The antimicrobial activities were carried out using cultures of *Staphylococcus aureus* as a Gram-positive bacterium and *Escherichia coli* as a Gram-negative bacterium. A solution of 20 mg mL^{-1} of each compound (free ligand, metal complexes and the standard drug *tetracycline*) in DMSO was prepared for testing. Centrifuged pellets of bacteria from a 24 h old culture containing approximately 10^4–10^6 CFU mL^{-1} (colony forming unit) were spread on the surface of Mueller Hinton agar plates. Then the wells were seeded with 10 mL of the prepared inocula to have 10^6 CFU mL^{-1}. Petri plates were prepared by pouring 100 mL of seeded nutrient agar. DMSO (0.1 mL) alone was used as the control under the same conditions for each microorganism, subtracting the diameter of the inhibition zone resulting with DMSO from that obtained in each case. The antimicrobial activities could be calculated as the mean of three replicates.

Acknowledgements

I thank Dr Krzysztof Radacki, Julius-Maximilians-Universität Würzburg, Germany, for refining the crystal structure of compound **3**.

References

1 (*a*) A. Korolkovas and J. H. Burckhalter, *Química Farmacêutica*, Guanabara Koogan, Rio de Janeiro, 1988, pp. 193–195; (*b*) R. N. Brogden, *Drugs*, 1986, **32**(Suppl. 4), 60–70; (*c*) A. Wong, A. Sibbald, F. Ferrero, M. Plager, M. E. Santolaya, A. M. Escobar, S. Campos, S. Barragan, M. De Leon Gonzalez and G. L. Kesselring, *Clin. Pediatr.*, 2001, **40**, 313–324.
2 H. Ergun, I. H. Ayhan and F. C. Tulunay, *Gen. Pharmacol.*, 1999, **33**, 237–241.
3 C. Muriel-Villoria, E. Zungri-Telo, M. Diaz-Curiel, M. Fernandez-Guerrero, J. Moreno, J. Puerta and P. Ortiz, *Eur. J. Clin. Pharmacol.*, 1995, **48**, 103–107.
4 W. Martindale and K. Parfitt, *The Complete Drug Reference*, Pharmaceutical Press, London, 32nd edn, 1999.
5 E. Zylber-Katz, L. Granit and M. Levy, *Eur. J. Clin. Pharmacol.*, 1992, **42**, 187–191.
6 (*a*) S. Z. Qureshi, A. Saeed and T. Hasan, *Talanta*, 1989, **36**(8), 869–871; (*b*) N. V. Pathak and I. C. Shukla, *J. Indian Chem. Soc.*, 1983, **60**, 206–207.
7 T. Perez-Ruiz, C. Martinez-Lozano, V. Tomas and J. Carpena, *Microchem. J.*, 1993, **47**, 296–301.
8 N. H. Eddine, F. Bressolle, B. Mandrou and H. Fabre, *Analyst*, 1982, **107**, 67–70.
9 (*a*) T. Pkrez-Ruiz, C. Martinez-Lozano and V. Tomas, *J. Pharm. Biomed. Anal.*, 1994, **12**(9), 1109–1113; (*b*) L. H. Marcolino-Júnior, M. F. Bergamini, M. F. S. Teixeira, E. T. G. Cavalheiro and O. Fatibello-Filho, *II Farmaco*, 2003, **58**, 999–1004.
10 F. Belal, *Electroanalysis*, 1992, **4**, 589.
11 F. Marchetti, C. Pettinari and R. Pettinari, *Coord. Chem. Rev.*, 2005, **249**, 2909–2945.
12 J. S. Casas, M. S. García-Tasende, A. Sánchez, J. Sordo and A. Touceda, *Coord. Chem. Rev.*, 2007, **251**(11–12), 1561–1589.
13 S. V. Tatwawadi, A. P. Singh and K. K. Narang, *Indian J. Chem., Sect. A: Inorg., Bio-inorg., Phys., Theor. Anal. Chem.*, 1982, **21A**(6), 644–645.
14 (*a*) R. C. Maurya and S. Rajput, *Synth. React. Inorg. Met.-Org. Chem.*, 2003, **33**(10), 1877–1894; (*b*) R. C. Maurya, N. Chturvedi and S. K. Thakur, *J. Inst. Chem.*, 1999, **71**(6), 216–220; (*c*) R. C. Maurya, V. Pillai and S. Rajput, *Synth. React. Inorg. Met.-Org. Chem.*, 2003, **33**(4), 699–716; (*d*) R. C. Maurya, D. K. Shrivastava and T. Singh, *J. Inst. Chem.*, 1999, **71**(5), 198–201; (*e*) R. C. Maurya and D. D. Mishra, *Synth. React. Inorg. Met.-Org. Chem.*, 1988, **18**(2), 133–140; (*f*) R. C. Maurya, R. Verma and B. Shukla, *Indian J. Chem., Sect. A: Inorg., Bio-inorg., Phys., Theor. Anal. Chem.*, 1999, **38**(7), 730–735; (*g*) R. C. Maurya, J. Dubey and B. Shukla, *Synth. React. Inorg. Met.-Org. Chem.*, 1998, **28**(7), 1159–1171; (*h*) R. C. Maurya, D. D. Mishra, P. K. Trivedi and A. Gupta, *Synth. React. Inorg. Met.-Org. Chem.*, 1994, **24**(1), 17–28; (*i*) R. C. Maurya, D. D. Mishra and S. Pillai, *Synth. React. Inorg. Met.-Org. Chem.*, 1997, **27**(10), 1453–1466; (*j*) R. C. Maurya, D. D. Mishra and V. Pillai, *Synth. React. Inorg. Met.-Org. Chem.*, 1995, **25**(7), 1127–1141; (*k*) R. C. Maurya, D. D. Mishra and V. Pillai, *Synth. React. Inorg. Met.-Org. Chem.*, 1995, **25**(1), 139–150; (*l*) R. C. Maurya, D. D. Mishra, S. Mukherjee and P. K. Trivedi, *Transition Met. Chem.*, 1991, **16**(5), 524–527.
15 N. N. Shaforostova, N. A. Skorik and E. N. Naprienko, *Zh. Neorg. Khim.*, 2000, **45**(8), 1344–1349.
16 O. A. Gabrichidze, *Koord. Khim.*, 1988, **14**(12), 1632–1635.
17 M. G. Miles, G. Doyle, R. P. Cooney and R. S. Tobias, *Spectrochim. Acta, Part A*, 1969, **25**, 1515–1526.
18 T. B. Chenskaya, M. Berghahn, P. C. Kunz, W. Frank and W. Kläui, *J. Mol. Struct.*, 2007, **829**, 135–148.
19 M. V. Marinho, L. F. Marques, R. Diniz, H. O. Stumpf, L. C. Visentin, M. I. Yoshida, F. C. Machado, F. Lioret and M. Julve, *Polyhedron*, 2012, **45**, 1–8.
20 A. B. P. Lever, *Inorganic Electronic Spectroscopy*, Elsevier, Amsterdam, 2nd edn, 1982.
21 A. Cotton and G. Wilkinson, *Advanced Inorganic Chemistry*, 2nd edn, 1972.
22 E. González, A. Rodrigue-Witchel and C. Reber, *Coord. Chem. Rev.*, 2007, **251**, 351–363.
23 A. Seminara, A. Musumeci and R. P. Bonomo, *Inorg. Chim. Acta*, 1984, **90**, 9–15.
24 N. T. Abdel-Ghani, M. F. Abo El-Ghar and A. M. Mansour, *Spectrochim. Acta, Part A*, 2013, **104**, 134–142.
25 J. A. Welleman, F. B. Hulsbergen, J. Verbiest and J. Reddijk, *J. Inorg. Nucl. Chem.*, 1978, **40**, 143–147.
26 R. J. Rudley and B. J. Hathaway, *J. Chem. Soc.*, 1970, 1725–1728.

27 B. J. Hathaway and D. E. Billing, *Coord. Chem. Rev.*, 1970, **5**, 143–207.
28 (*a*) A. E. Reed, L. A. Curtiuss and F. Weinhold, *Chem. Rev.*, 1988, **88**, 899; (*b*) A. M. Mansour, *Inorg. Chim. Acta*, 2013, **408**, 186–192.
29 A. M. Mansour, *Inorg. Chim. Acta*, 2013, **394**, 436–445.
30 A. M. Mansour, *Spectrochim. Acta, Part A*, 2014, **123**, 257–266.
31 B. Tweedy, *Phytopathology*, 1964, **55**, 910.
32 J. Pons, A. Chadghan, J. Casabó, A. Alvarez-Larena, J. Francesc Piniella and J. Ros, *Polyhedron*, 2001, **20**, 2531.
33 A. L. Spek, *J. Appl. Crystallogr.*, 2003, **36**, 7–13.
34 A. L. Spek, *Program for reduction of CAD-4 Data*, University of Utrecht, The Netherlands, 1996.
35 A. Altomare, G. Cascarano, C. Giacovazzo, A. Guagliardi, M. C. Burla, G. Polidori and M. Camalli, *J. Appl. Crystallogr.*, 1994, **27**, 435–436.
36 G. M. Sheldrick, *Acta Crystallogr., Sect. A: Fundam. Crystallogr.*, 2008, **64**, 112.
37 C. K. Johnson, ORTEP—II. A Fortran Thermal—Ellipsoid Plot Program. Report ORNL-5138. Oak Ridge National Laboratory, Oak Ridge, Tennessee, USA, 1976.
38 A. M. Mansour, *Polyhedron*, 2014, **78**, 10–17.
39 M. J. Frisch, G. W. Trucks, H. B. Schlegel, G. E. Scuseria, M. A. Robb, J. R. Cheeseman, V. G. Zakrzewski, J. A. Montgomery, R. E. Stratmann, J. C. Burant, S. Dapprich, J. M. Millam, A. D. Daniels, K. N. Kudin, M. C. Strain, O. Farkas, J. Tomasi, V. Barone, M. Cossi, R. Cammi, B. Mennucci, C. Pomelli, C. Adamo, S. Clifford, J. Ochterski, G. A. Petersson, P. Y. Ayala, Q. Cui, K. Morokuma, D. K. Malick, A. D. Rabuck, K. Raghavachari, J. B. Foresman, J. Cioslowski, J. V. Ortiz, A. G. Baboul, B. B. Stefanov, G. Liu, A. Liashenko, P. Piskorz, I. Komaromi, R. Gomperts, R. L. Martin, D. J. Fox, T. Keith, M. A. Al-Laham, C. Y. Peng, A. Nanayakkara, C. Gonzalez, M. Challacombe, P. M. W. Gill, B. G. Johnson, W. Chen, M. W. Wong, J. L. Andres, M. Head-Gordon, E. S. Replogle and J. A. Pople, *GAUSSIAN 03 (Revision A.9)*, Gaussian, Inc., Pittsburgh, 2003.
40 N. T. Abdel-Ghani and A. M. Mansour, *J. Coord. Chem.*, 2012, **65**(5), 763–779.
41 N. T. Abdel-Ghani and A. M. Mansour, *Eur. J. Med. Chem.*, 2012, **47**, 399.
42 National Committee for Clinical Laboratory Standards, *NCCLS Approval Standard Document M2-A7*, Villanova, PA, 2000.